Theory of proximity-effect sandwiches with magnetic impurities

M. J. DeWeert and Gerald B. Arnold
Department of Physics, University of Notre Dame, Notre Dame, Indiana 46556
(Received 12 March 1984)

We extend the theory of proximity-effect sandwiches consisting of a thin normal (N) metal in perfect planar contact with a thick superconducting (S) metal to the case in which the N metal contains magnetic as well as nonmagnetic impurities. We consider dilute concentrations of antiferromagnetic impurities, adapting the theory of Zittartz, Bringer, and Müller-Hartmann for magnetic impurities in superconductors to proximity systems. We discuss the influences of Kondo-effect impurities in this proximity system. We compare our theory with the experimental results of Dumoulin, Guyon, and Nedellec, and suggest possible cases in which new phenomena, such as the presence of three gaps in the density of states, might be observed.

I. INTRODUCTION

There has recently been much interest in proximity-effect sandwiches containing Kondo-effect impurities. Other theoretical efforts[1,2] concerning these systems have assumed the validity of the McMillan tunneling model. We consider here a thin N metal in perfect planar contact with a thick clean S metal. Since the McMillan model assumes a tunneling barrier between N and S, it is not strictly applicable to this situation. We base our treatment here on two previous papers[3,4] and shall use theories by Maki[5] and Zittartz, Bringer, and Müller-Hartmann[6] to modify these results for the case in which the N metal contains dilute magnetic impurities.

This work represents the first treatment of magnetic impurities in the N metal of an N-S double-layer system in which the N-S interface is transparent in the normal state. This transparency (or near transparency) appears to be far more common experimentally than the situation required by the McMillan tunneling model for an N-S double layer. We find that the density of states for tunneling into the N side displays states below the S-metal energy gap. These states arise from a "resonant depairing" which occurs via scattering of quasiparticles from the Kondo impurities. For sufficiently thick N metal, we also find a novel regime in which the tunneling density of states displays *three* gaps, created by the simultaneous existence of a proximity-effect-related bound state and the Kondo-effect bound state.

Our approach is to approximate the self-energy Σ as a sum of phonon and impurity terms: $\Sigma(x)=\Sigma^{\rm ph}(x)+\Sigma^{nm}(x)+\Sigma^{m}(x)$. We assume as in Refs. 3 and 4 (hereafter referred to as PE I and PE II, respectively) that Σ is a local function, and further that it depends only on x, the coordinates parallel to the interface having been Fourier transformed away. Diagrammatically, this approximation is represented in Fig. 1. The nonmagnetic scattering self-energy Σ^{nm} represents an average over all the impurities. The magnetic scattering self-energy Σ^{m} is not simply represented diagrammatically, but again all its internal energies and pair potentials are to be fully dressed, renormalized by the proximity effect and nonmagnetic scattering as well.

Our ansatz for Σ is

$$\Sigma=\begin{bmatrix}[1-Z(x)]E & \phi(x)\\ \phi(x) & [1-Z(x)]E\end{bmatrix},$$

so that $Z(x)$ and $\phi(x)$ are given by

$$\begin{aligned}Z(x)&=Z^{\rm ph}(x)+Z^{nm}(x)+Z^{m}(x)\,,\\ \phi(x)&=\phi^{\rm ph}(x)+\phi^{nm}(x)+\phi^{m}(x)\,,\end{aligned}\tag{1.1}$$

where Z is the renormalization function and ϕ is the pairing self-energy. The pair potential $\Delta(x)$ is given by $\phi(x)/Z(x)$. Our expressions for $\phi^{\rm ph}(x)$ and $Z^{\rm ph}(x)$ come from PE I, where the case of perfectly clean metals was considered [see Eqs. (6.5) and (6.6) of PE I]:

$$\begin{aligned}\phi^{\rm ph}(E,x)&=\int_0^\infty dE' f(E',x)K_+(E,E',x)\,,\\ EZ^{\rm ph}(E,x)&=E-\int_0^\infty dE' N(E',x)K_-(E,E',x)\,,\end{aligned}\tag{1.2}$$

where $f(E,x)$ is the local pair density of states, $N(E,x)$ is the local normalized density of states and $K_\pm(E,E',x)$ are the local electron-phonon interaction kernels. In PE II, elastic scattering from defects or nonmagnetic impurities was accounted for by adding to the interaction kernels terms of the form [see Eq. (1.13) of PE II]:

$$K_\pm^{\rm imp}(E,E',x)=\pm\frac{i\hbar}{2\tau(x)}\delta(E-E')\,,\tag{1.3}$$

which yielded

$$\begin{aligned}\phi^{nm}(E,x)&=\frac{i\hbar}{2\tau(x)}f(E,x)\,,\\ Z^{nm}(E,x)&=-\frac{i\hbar}{2\tau(x)}N(E,x)\,.\end{aligned}\tag{1.4}$$

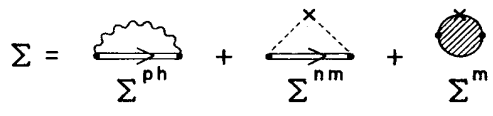

FIG. 1. Approximation to the self-energy.

As we shall see, $\phi^m(E,x)$ and $Z^m(E,x)$ are also given by simple-looking expressions, though the diagrammatic representation of Σ^m is not simple.

II. BULK SUPERCONDUCTORS WITH MAGNETIC IMPURITIES

Since we have assumed Σ to be local, we will examine models of magnetic impurities in bulk superconductors which assumed local interactions between electrons and impurities and we use them as guides in obtaining $\Sigma^m(x)$.

A. The Maki theory

Maki assumed the self-consistent Born approximation for scattering from both magnetic and nonmagnetic impurities, so that Σ^m diagrammatically resembles Σ^{nm} in Fig. 1. His approximation yielded

$$\Sigma^{\text{imp}}=\begin{bmatrix} -\left[\frac{i\hbar}{2\tau_1}+\frac{i\hbar}{2\tau_2}\right]N(E) & \left[\frac{i\hbar}{2\tau_1}-\frac{i\hbar}{2\tau_2}\right]f(E) \\ \left[\frac{i\hbar}{2\tau_1}-\frac{i\hbar}{2\tau_2}\right]f(E) & -\left[\frac{i\hbar}{2\tau_1}+\frac{i\hbar}{2\tau_2}\right]N(E) \end{bmatrix}, \tag{2.1}$$

where τ_1 and τ_2 are the lifetimes for scattering for nonmagnetic and magnetic impurities, and $N(E)$ and $f(E)$ are given in bulk metals by

$$N(E)=E/(E^2-\Delta^2)^{1/2},$$
$$f(E)=\Delta/(E^2-\Delta^2)^{1/2}.$$

The most important feature of this self-energy is that τ_2 appears in the diagonal and off-diagonal terms with opposite signs relative to τ_1. This leads to gapless superconductivity as τ_2 becomes small.

B. The theory of Zittartz, Bringer, and Müller-Hartmann

It is well known, however, that the Born approximation is insufficient to explain the Kondo effects. Using a self-consistent transition-matrix approximation, Zittartz, Bringer, and Müller-Hartmann[7–9] obtained a solution for the Green function of a bulk superconductor with s-wave scattering by magnetic impurities. The Hamiltonian of their system is local and leads to a local (that is, momentum-independent) transition matrix T. In Ref. 9, it is shown that for energies near the Fermi energy, the T matrix may be approximated by simple functions. In Ref. 6, hereafter referred to as ZBMH, the self-energy Σ is identified with T, an approximation which is correct to first order in the impurity concentration, and the bulk density of states is elucidated.

The self-energy of ZBMH is given by

$$\Sigma^m\cong T\cong\frac{i\hbar\gamma}{\tau_2}(1-y_0)\frac{(E^2-\Delta^2)^{1/2}}{(E^2-y_0^2\Delta^2)}\begin{bmatrix} E & -y_0\Delta \\ -y_0\Delta & E \end{bmatrix}, \tag{2.2}$$

where we have translated the ZBMH notation into our own. Here y_0 and γ contain the parameters of the Kondo effect. There exists a bound state of an energy E_0, and $y_0=E_0/\Delta$ gives its position relative to the energy gap. The other parameters are hidden in γ:

$$\gamma\equiv 2/[\pi^2N_0^2J^2S(S+1)]. \tag{2.3}$$

Here N_0 is the density of states per spin at the Fermi surface, S is the impurity spin, and J is the strength of interaction between the impurity and the conduction electrons. In this simple model, J was assumed to be constant up to some cutoff energy D, above which it vanished. Antiferromagnetic coupling ($J<0$) leads to $0<y_0<1$, and is the case of interest here. Ferromagnetic coupling gives $y_0>1$, but according to Müller-Hartmann,[10] E_0 then separates very little from Δ, so this case is less interesting.

In terms of the fundamental quantities of the system, y_0 is given by (see Eq. 2 of Ref. 6):

$$y_0=\left[1-\frac{\pi^2S(S+1)}{\alpha^2+\pi^2S(S+1)}\right]^{1/2},$$
$$\alpha\equiv\ln[(\beta_cD)e^{1/JN_0}]=\ln(T_k/T_c)\quad(J<0), \tag{2.4}$$

where $2D$ is the width of the impurity band, T_k is the Kondo temperature, and $\beta_c=(k_BT_c)^{-1}$.

The validity of perturbation theory relies on $\ln(\beta_cD)$ being small. Then we have $\alpha\cong(JN_0)^{-1}$, and as $J\to 0$, $y_0\to 1$ and $(1-y_0)\to[\frac{1}{2}\pi^2S(S+1)J^2N_0^2]$, so that $b(E)\to 1$ and the results of Maki are recovered. The exact correspondence between this work and that of ZBMH is made by identifying

$$\frac{\hbar}{\tau_2}\equiv 4\pi cN_0J^2S(S+1)=\frac{8c}{N_0\gamma}, \tag{2.5}$$

where c is the impurity concentration.

Equation (2.4) may be inverted to give J in terms of y_0 and so to eliminate J from Eq. (2.3) for γ. This yields

$$\gamma=2\left[\frac{y_0^2}{1-y_0^2}-\frac{\ln(\beta_cD)}{\pi\sqrt{S(S+1)}}\right]. \tag{2.6}$$

Assuming $1>y_0>0$ and $\ln(\beta_cD)$ small, we thus obtain

$$\frac{b(E)}{\tau_2}\cong\frac{1}{\tau_2}\frac{2y_0^2}{1+y_0}\frac{E^2-\Delta^2}{E^2-y_0^2\Delta^2}\times\begin{cases}1, & \text{diagonal}\\ y_0, & \text{off diagonal}\end{cases} \tag{2.7}$$

and

$$\frac{\hbar}{\tau_2}\cong\frac{4c}{\pi N_0}\frac{1-y_0^2}{y_0^2}, \tag{2.8a}$$

$$\frac{d}{l_2}=\frac{1}{2}R\frac{\hbar}{\tau_2}=\frac{2Rc}{\pi N_0}\frac{1-y_0^2}{y_0^2}. \tag{2.8b}$$

C. Comparison of Maki and ZBMH theories

The ZBMH theory differs markedly from that of Maki in bulk materials. Whereas Maki's results predict merely a lowering of the energy gap in the density of states, ZBMH predicts the appearance of a "bound state" in the energy gap near $E_0=y_0\Delta$. There are thus two energy

gaps possible in the density of states. Only for J small and impurity concentrations so large that the bound state merges with the continuum ($y_0 \to 1$) are the results of Maki recovered.

III. ADAPTATION OF ZBMH TO PROXIMITY GEOMETRIES

We must modify $\Sigma^m_{\rm bulk}(E)$ to obtain the correct self-energy for the proximity system. In bulk superconductors, we may identify

$$G_{11}(E) \propto N_{\rm bulk} = E/[E^2-\Delta^2(E)]^{1/2} , \tag{3.1a}$$

$$G_{12}(E) \propto f_{\rm bulk} = \Delta(E)/[E^2-\Delta^2(E)]^{1/2} , \tag{3.1b}$$

so that for the magnetic self-energy we have from Eq. (2.2)

$$\Sigma^m_{\rm bulk}(E) = \frac{i\hbar}{\tau_2}\frac{2y_0}{1+y_0}\frac{1}{N^2(E)-y_0^2 f^2(E)} \times \begin{bmatrix} N(E) & -y_0 f(E) \\ -y_0 f(E) & N(E) \end{bmatrix} . \tag{3.2}$$

However, self-consistency requires that we use not G_{11} and G_{12} for bulk metals, but for the proximity geometry instead. Furthermore, we are tunneling into the N-metal side of the sandwich, so we need $N_N(E)$ and $f_N(E)$, given by [see Eqs. (2.1)–(2.8) of PE II]

$$f_N(E,x) = i\left[\frac{\Delta_N}{\Omega_N}\chi_1(E) + \frac{E}{\Omega_N}\chi_2(E,x)\right] , \tag{3.3}$$

$$N_N(E,x) = i\left[\frac{E}{\Omega_N}\chi_1(E) + \frac{\Delta_N}{\Omega_N}\chi_2(E,x)\right] , \tag{3.4}$$

where $\Omega_{N,S} = (E^2-\Delta^2_{N,S})^{1/2}$, and

$$\chi_1(E) = \frac{iF(E)\cos(\Delta K^N d)+\sin(\Delta K^N d)}{iF(E)\sin(\Delta K^N d)-\cos(\Delta K^N d)} , \tag{3.5}$$

$$\chi_2(E,x) = \frac{i\cos[\Delta K^N(x+d)]G(E)}{iF(E)\sin(\Delta K^N d)-\cos(\Delta K^N d)} , \tag{3.6}$$

$$F(E) = (E^2-\Delta_S\Delta_N)/\Omega_S\Omega_N , \tag{3.7}$$

$$G(E) = E(\Delta_S-\Delta_N)/\Omega_S\Delta\Omega_N , \tag{3.8}$$

and

$$\Delta K^N = 2Z_N(E)\Omega_N/\hbar v_F\cos\theta . \tag{3.9}$$

As in PE II, θ is the angle between the normal to the N-S interface and the $\vec{k}$ vector of the incident electron. In correspondence with PE II, we now have

$$\phi^m_N(E) = -\frac{i\hbar}{2\tau_2}y_0\langle b(E)f(E,x)\rangle_N , \tag{3.10a}$$

$$EZ^m_N(E) = \frac{i\hbar}{2\tau_2}\langle b(E)N(E,x)\rangle_N , \tag{3.10b}$$

where

$$b(E) = \frac{2y_0^2}{1+y_0}\frac{1}{N^2(E,x)-y_0^2 f^2(E,x)} \tag{3.11}$$

and the angular brackets denote an average over the thickness of the normal metal. Since the N metal is assumed to be thin, ϕ and Z should vary little from their average values. Thus for the total ϕ_N and Z_N we have

$$\phi_N(E) = \phi^{\rm ph}_N(E) + \frac{i\hbar}{2\tau_1}\langle f(E,x)\rangle_N - \frac{i\hbar}{2\tau_2}y_0\langle b(E,x)f(E,x)\rangle_N , \tag{3.12}$$

$$EZ_N(E) = EZ^{\rm ph}_N(E) + \frac{i\hbar}{2\tau_1}\langle N(E,x)\rangle_N + \frac{i\hbar}{2\tau_2}\langle b(E,x)N(E,x)\rangle_N . \tag{3.13}$$

Inserting Eqs. (3.3) and (3.4) into (3.11) through (3.13) now yields

$$\phi_N(E) = \phi^{\rm ph}_N(E) - \frac{\hbar}{2}\int_{-d}^{0}\frac{dx}{d}\int_0^1 d(\cos\theta)\left[\frac{1}{\tau_1}-\frac{y_0 b(E)}{\tau_2}\right]\left[\frac{\Delta_N}{\Omega_N}\chi_1(E)+\frac{E}{\Omega_N}\chi_2(E,x)\right] , \tag{3.14}$$

$$Z_N(E) = Z^{\rm ph}_N(E) = \frac{\hbar}{2E}\int_{-d}^{0}\frac{dx}{d}\int_0^1 d(\cos\theta)\left[\frac{1}{\tau_1}+\frac{b(E)}{\tau_2}\right]\left[\frac{E}{\Omega_N}\chi_1(E)+\frac{\Delta_N}{\Omega_N}\chi_2(E,x)\right] , \tag{3.15}$$

and

$$b(E,x) = \frac{2y_0^2}{1+y_0}\frac{\Omega_N^2}{-\chi_1^2(E)(E^2-y_0^2\Delta_N^2)-2\chi_1(E)\chi_2(E,x)E\Delta_N(1-y_0^2)+\chi_2^2(E,x)(y_0^2E^2-\Delta_N^2)} . \tag{3.16}$$

Together, Eqs. (3.14)–(3.16) present a somewhat formidable set. We begin approximating them by replacing $\chi_2(E,x)$ in Eq. (3.16) with

$$\chi_2(E) = \int_{-d}^{0}\frac{dx}{d}\int_0^1 d(\cos\theta)\chi_2(E,x) ,$$

so that $b(E,x) = b(E)$ and may be taken outside the integral signs in Eqs. (3.14) and (3.15). At the energies of interest, the spatial variations of all relevant quantities are over a coherence distance, so this averaging has little effect. We then use $\Delta_N(E)Z_N(E) = \phi_N(E)$ to obtain an expression for $\Delta_N(E)$:

$$\Delta_N(E)=\left\{\Delta_N^{\rm ph}(E)+\frac{db(E)}{l_2}\frac{(1+y_0)\Delta_N}{RZ_N^{\rm ph}\Omega_N}\int_{-d}^{0}\frac{dx}{d}\int_0^1 d(\cos\theta)\chi_1(E)\right.$$
$$\left.+\frac{1}{RZ_N^{\rm ph}\Omega_N E}\int_{-d}^{0}\frac{dx}{d}\int d(\cos\theta)\left[\Delta_N^2\left[\frac{db(E)}{l_2}+\frac{d}{l_1}\right]+E^2\left[\frac{db(E)}{l_2}y_0-\frac{d}{l_1}\right]\right]\chi_2(E,x)\right\}, \tag{3.17}$$

where $R=2d/\hbar v_F$ and $l_j=\tau_j v_F$. We could in principle now solve Eqs. (3.15)–(3.17) self-consistently for $Z_N(E)$ and $\Delta_N(E)$. However, the equations are quite complex, and, as we shall see, may have degenerate solutions. One limit in which we can solve (3.17) exactly for $\Delta_N(E)$ is that in which $\Delta K^N d$ has a large imaginary part. Then $\sin(\Delta K^N d)\cong i\cos(\Delta K^N d)$, and

$$\chi_1(E)=-i\ , \tag{3.18}$$

$$\chi_2(E,x)=\frac{G(E)}{F(E)+1}\frac{\cos[\Delta K^N(x+d)]}{\sin(\Delta K^N d)}\ , \tag{3.19}$$

$$\chi_2(E)=\int_{-d}^{0}\frac{dx}{d}\int_0^1 d(\cos\theta)\chi_2(E,x)=\frac{1}{2}\frac{G(E)}{RZ_N\Omega_N(F(E)+1)}\ . \tag{3.20}$$

We then have from Eq. (3.15):

$$RZ_N\Omega_N=RZ_N^{\rm ph}\Omega_N-\left[\frac{d}{l_1}+\frac{db(E)}{l_2}\right]\int_{-d}^{0}\frac{dx}{d}\int_0^1 d(\cos\theta)\left[-i+\frac{\Delta_N(\Delta_S-\Delta_N)\cos\Delta K^N(x+d)}{(E^2-\Delta_S\Delta_N+\Omega_S\Omega_N)\sin(\Delta K^N d)}\right]$$
$$\cong i\left[\frac{d}{l_1}+\frac{d}{l_2}b(E)\right]. \tag{3.21}$$

Since $RZ_N\Omega_N=\Delta K^N d\cos\theta$, we see that d/l_1 large will usually be sufficient to guarantee $\mathrm{Im}(\Delta K^N d)$ large, excepting the small fraction of quasiparticles for which $\cos\theta$ is small.

Substituting (3.16) through (3.21) into (3.16) gives us an approximation for $b(E)$:

$$b(E)\cong\left[\frac{2y_0^2}{1+y_0}\right]\left[\frac{\Omega_N^2}{(E^2-y_0^2\Delta_N^2)+\dfrac{i\Delta_N E^2(\Delta_S-\Delta_N)}{RZ_N\Omega_N(E^2-\Delta_S\Delta_N+\Omega_S\Omega_N)}+\dfrac{(y_0^2E^2-\Delta_N^2)E^2(\Delta_S-\Delta_N)^2}{4(RZ_N\Omega_N)^2(E^2-\Delta_S\Delta_N+\Omega_S\Omega_N)^2}}\right]$$
$$\cong\frac{2y_0^2}{1+y_0}\frac{\Omega_N^2}{\Omega_{N_0}^2}\ , \tag{3.22}$$

where $\Omega_{N_0}=(E^2-y_0^2\Delta_N^2)^{1/2}$, and we have assumed $|RZ_N\Omega_N|$ to be large. From (3.22) we see that (3.21) potentially has a zero regardless of how large d/l_1 may be. This zero occurs at an energy

$$E_r=y_0\Delta_N\left[\frac{\dfrac{d}{l_1}+\dfrac{2}{1+y_0}\dfrac{d}{l_2}}{\dfrac{d}{l_1}+\dfrac{2y_0^2}{1+y_0}\dfrac{d}{l_2}}\right]^{1/2}. \tag{3.23}$$

There is no cause for abandoning our assumption that $\mathrm{Im}(\Delta K^N d)$ is large, however. It will turn out that for $E>0$, Δ_N always has a large imaginary part in the vicinity of $E=y_0\mathrm{Re}(\Delta_N)$, so that (3.23) cannot be satisfied. In any case, if we were concerned with large d/l_1 and small d/l_2, the region over which (3.23) is approximately satisfied would be quite small and we could neglect it.

IV. SOLUTION FOR $\Delta_N(E)$

A. Basic equations

Using (3.22) for $b(E)$, we obtain expressions for $RZ_N\Omega_N$ and $\Delta_N(E)$ from Eqs. (3.21) and (3.17):

$$RZ_N(E)\Omega_N\cong i\left[\frac{d}{l_1}+\frac{d}{l_2}\frac{2y_0^2}{1+y_0}\frac{\Omega_N^2}{\Omega_{N_0}^2}\right], \tag{4.1}$$

$$\Delta_N(E)\cong\Delta_N^{\rm ph}-i\frac{d}{l_2}\frac{2y_0^2\Delta_N\Omega_N}{RZ_N^{\rm ph}\Omega_{N_0}^2}+\frac{i(\Delta_S-\Delta_N)\Omega_N}{2RZ_N^{\rm ph}(E^2-\Delta_S\Delta_N+\Omega_S\Omega_N)}\frac{E^2\left[\frac{d}{l_1}-\frac{2y_0^3}{1+y_0}\frac{d}{l_2}\right]-y_0^2\Delta_N^2\left[\frac{d}{l_1}+\frac{2}{1+y_0}\frac{d}{l_2}\right]}{-E^2\left[\frac{d}{l_1}+\frac{2y_0^2}{1+y_0}\frac{d}{l_2}\right]-y_0^2\Delta_N^2\left[\frac{d}{l_1}+\frac{2}{1+y_0}\frac{d}{l_2}\right]}$$

$$=\Delta_N^{\rm ph}-2i\frac{d}{l_2}\frac{y_0^2\Delta_N\Omega_N}{RZ_N^{\rm ph}\Omega_{N_0}^2}+\frac{i(\Delta_S-\Delta_N)\Omega_N}{2RZ_N^{\rm ph}(E^2-\Delta_S\Delta_N+A_SA_N)}\frac{r_1E^2-y_0^2\Delta_N}{r_2E^2-y_0^2\Delta_N^2}\,, \tag{4.2}$$

where

$$r_1\equiv\left[\frac{d}{l_1}-\frac{2y_0^3}{1+y_0}\frac{d}{l_2}\right]\Big/\left[\frac{d}{l_1}+\frac{2}{1+y_0}\frac{d}{l_2}\right], \tag{4.3}$$

and

$$r_2\equiv\left[\frac{d}{l_1}+\frac{2y_0^2}{1+y_0}\frac{d}{l_2}\right]\Big/\left[\frac{d}{l_1}+\frac{2}{1+y_0}\frac{d}{l_2}\right]. \tag{4.4}$$

B. Analytic limits

There are few limits in which simple analytic solutions to (4.2) are possible, but these are quite useful. The first limit is $E=0$. Then we have

$$0=(y_0\Delta_N)^2\left[\Delta_N(4RZ_N^{\rm ph}\Delta_S+1)-\Delta_S\left[4RZ_N^{\rm ph}\Delta_N^{\rm ph}+1-8\frac{d}{l_2}\right]\right]. \tag{4.5}$$

We see that $\Delta_N=0$ is always a root at $E=0$. It is the correct root to take when the other solution to (4.5) gives $\Delta_N<0$, for we exclude pair potentials with negative real parts as unphysical. Thus we have

$$\Delta_N(E=0)=\begin{cases}\Delta_S\dfrac{4RZ_N^{\rm ph}\Delta_N^{\rm ph}+1-8\frac{d}{l_2}}{4RZ_N^{\rm ph}\Delta_S+1} & \text{for } \Delta_N>0\\ 0 \quad \text{otherwise}\,.\end{cases} \tag{4.6}$$

A second useful analytic limit is $E=\Delta_S$. In this case, $\Delta_N=\Delta_S$ is always a solution. The other roots are difficult to extract analytically, being solutions to a fifth-order polynomial in Δ_N.

Finally, we consider the limit of very large energy. For $E\gg\Delta_{S,N}$, negligible $\phi_N^{\rm ph}$, and $\Delta_N^{\rm ph}$, $RZ_N^{\rm ph}E$, and d/l_2 small, Eq. (4.2) reduces to

$$\Delta_N(E)\cong\frac{\Delta_S-i4RZ_N^{\rm ph}E\Delta_N^{\rm ph}(r_2/r_1)}{1-[i4RZ_N^{\rm ph}E-8(d/l_2)y_0^2](r_2/r_1)}$$

$$\cong\Delta_S e^{(r_2/r_1)[i4RZ_N^{\rm ph}E-8(d/l_2)y_0^2]}\,. \tag{4.7}$$

Thus we again have the homogenization of the pair potential as $RZ_N^{\rm ph}E$ vanishes as found in PE II. Furthermore, the oscillatory behavior persists, though its frequency is altered by a factor of r_2/r_1 (which is greater than unity) and its amplitude decreased by $e^{-8(d/l_2)y_0^2(r_2/r_1)}$.

C. General solution for $\Delta_N(E)$

At first approach, Eq. (4.2) for $\Delta_N(E)$ is quite imposing. However, it is algebraically straightforward (though slightly tedious) to obtain a polynomial in Δ_N from it. Extracting an extraneous root $\Delta_N=\Delta_S$, we obtain an 11th degree polynomial in Δ_N. For given values of the input parameters R, $Z_N^{\rm ph}$, $\Delta_N^{\rm ph}$, Δ_S, l_1, l_2, y_0, and d, the polynomial was solved numerically for Δ_N at each energy of interest using an International Mathematics and Scientific Library (IMSL) routine.[11] Of the eleven roots generated at each energy, all with negative real parts were rejected. We then substituted the remaining roots into Eq. (4.2), which only two or three of them satisfied well. Requiring $\Delta_N(E)$ to be continuous (though not necessarily to have a continuous derivative) then yielded at most three distinct Δ_N-versus-E curves to discriminate among. This discrimination was made by requiring the integral of the density of states derived from $\Delta_N(E)$ to approximate unity, which was always sufficient to determine a unique solution.

D. Tunneling density of states

From Eqs. (4.2) and (4.5) of PE I we have the tunneling density of states at 0 K for specular tunneling:

$$N_T(E)=\mathrm{Re}\left[\frac{E}{\Omega_N}\frac{(E^2-\Delta_S\Delta_N)\cosh(-i\Delta K^N d)+\Omega_S\Omega_N\sinh(-i\Delta K^N d)+\Delta_N(\Delta_S-\Delta_N)}{(E^2-\Delta_S\Delta_N)\sinh(-i\Delta K^N d)-\Omega_S\Omega_N\cosh(-i\Delta_K^N d)}\right]. \tag{4.8}$$

Using Eq. (4.1) for $RZ_N\Omega_N$ and considering only $\theta=0$, we may approximate

$$N_T(E)=\mathrm{Re}\left[\frac{E}{\Omega_N}+\frac{\Delta_N E(\Delta_S-\Delta_N)}{\Omega_N(E^2+\Omega_S\Omega_N-\Delta_S\Delta_N)\sinh\left[\frac{d}{l_1}+\frac{d}{l_2}b(E)\right]}\right], \tag{4.9}$$

where we use (3.22) for $b(E)$.

For d_S infinite, Eq. (4.9) is correct, but for d_S large but finite $N_T(E)$ is better approximated by an expression due to Gallagher [see Eq. (3) of Ref. 12]:

$$N_T(E)=\mathrm{Re}\left[D\frac{E}{\Omega_S\Omega_N^2}(E^2-\Delta_S\Delta_N)\cosh(-i\Delta K^N d)\sin(\Delta K^S d)+i\Omega_S\Omega_N\sinh(-i\Delta K^N d)\cos(\Delta K^S d)\right.$$
$$\left.+\Delta_N(\Delta_S-\Delta_N)\sin(\Delta K^S d)\right],$$

where

$$D^{-2}=1-\left[\cosh(-i\Delta K^N d)\cos(\Delta K^S d)-i\frac{E^2-\Delta_S\Delta_N}{\Omega_S\Omega_N}\sinh(i\Delta K^N d)\sin(\Delta K^S d)\right]^2.$$

Identifying $\Delta K^S d$ as $R_S Z_S \Omega_S/\cos\theta$, considering only $\theta=0$ and again using Eq. (4.1) for $R_N Z_N \Omega_N$ yields

$$N_T(E)\cong\mathrm{Re}\left\{D\frac{E}{\Omega_S\Omega_N^2}\left[(E^2-\Delta_S\Delta_N)\cosh\left[\frac{d}{l_1}+\frac{d}{l_2}b(E)\right]\sin(R_S Z_S\Omega_S)\right.\right.$$
$$\left.\left.+i\Omega_S\Omega_N\sinh\left[\frac{d}{l_1}+\frac{d}{l_2}b(E)\right]\cos(R_S Z_S\Omega_S)+\Delta_N(\Delta_S-\Delta_N)\sin(R_S Z_S\Omega_S)\right]\right\} \quad (4.10)$$

with

$$D^{-2}\cong 1-\left[\cosh\left[\frac{d}{l_1}+\frac{d}{l_2}b(E)\right]\cos(R_S Z_S\Omega_S)-i\frac{E-\Delta_S\Delta_N}{\Omega_S\Omega_N}\sinh\left[\frac{d}{l_1}+\frac{d}{l_2}b(E)\right]\sin(R_S Z_S\Omega_S)\right]^2. \quad (4.11)$$

For $d_S \gg d_N$, the density of states given by (4.10) differs significantly from that given by (4.9) only at energies far above Δ_S.

V. THEORETICAL RESULTS AT ZERO TEMPERATURE

A. Variation of $\Delta_N(E)$ and $N_T(E)$ with concentration for fixed y_0

Figure 2 shows the variation of $\Delta_N(E)$ with the magnetic impurity concentration c for $y_0-0.23$, $\Delta_S=1.20$,

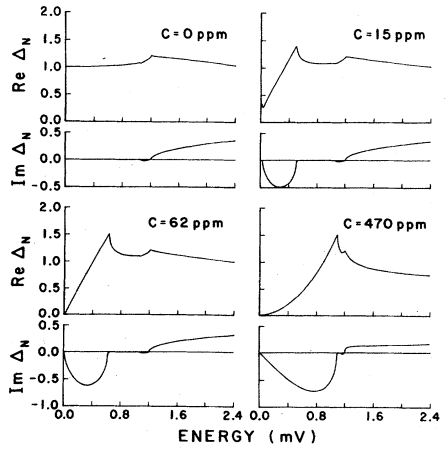

FIG. 2. N-metal pair potential versus the magnetic impurity concentration. Here we have assumed parameters approximately appropriate to 250 Å of copper evaporated on an S metal with $\Delta_S=1.2$ mV.

$Z_N^{\mathrm{ph}}=1.2$, and $R=0.0484$. This value of R would, for example, correspond to a 250-Å copper film, in which case the value of y_0 corresponds to a concentration of about 200 d/l_2 parts per million. We include the Δ_N-versus-E curve for the case considered in PE II, where only nonmagnetic impurities were present. We obtain d/l_2 from c via Eq. (2.8), and in this and all subsequent discussion we assume $d/l_1=3$, at which the effect of nonmagnetic impurity scattering seems to have saturated.

For small c, $\Delta_N(E)$ develops a negative imaginary part in the vicinity of $E=y_0\Delta_S$. Corresponding to this imaginary part, $\Delta_N(E)$ develops in its real part a linearly increasing region, and $\Delta_N(E=0)$ is depressed below its $c=0$ value. As c increases, the region of negative imaginary Δ_N broadens until its lower edge reaches $E=0$, at which point the real part of Δ_N also vanishes. Above the concentration at which $\Delta_N(E=0)=0$, the real part changes from a linear to a parabolic shape for $E<\Delta_S$. For extremely high c, $\mathrm{Re}[\Delta_N(E)]$ is flattened about $E=\Delta_S$, and $\mathrm{Im}[\Delta_N(E)]$ begins to vanish everywhere. As c becomes large, $\Delta_N(E)$ vanishes everywhere, which we expect for extremely large concentrations of magnetic impurities.

Physically, we have a scattering anomaly at $E=E_F\pm y_0\Delta_S$. In a bulk normal metal, the amplitude for scattering of electrons off the magnetic impurities has a logarithmic divergence at the Fermi surface. In a superconductor, the divergence is pulled to $\pm y_0\Delta$ away from the Fermi surface. Since the scattering can break Cooper pairs, they develop a finite lifetime, which is reflected in $\Delta_N(E)$ as a nonzero imaginary part.

We ascribe the energy-dependent structure below Δ_S in

Fig. 5 to "resonant depairing," a phenomenon peculiar to Kondo impurities in a superconductor. This phenomenon is merely the reverse of resonant pairing in a superconductor, whereby resonant phonon emission at some phonon energy initially enhances $\mathrm{Re}\Delta_N$ above its BCS value, but then causes a steady decrease in this quantity as the pair lifetime due to phonon emission decreases, eventually yielding a negative $\mathrm{Re}\Delta_N$ at energies far above the resonant energy. In resonant depairing, $\mathrm{Re}\Delta_N$ begins at the depressed value appropriate to standard nonresonant spin-flip scattering, but as the resonant energy ($y_0\Delta_S$) is approached, $\mathrm{Re}\Delta_N$ is initially further depressed, then *rises* gradually as the pair lifetime due to Kondo (resonant spin-flip) scattering decreases. $\mathrm{Re}\Delta_N$ then saturates at the value one would obtain if there were no spin-flip scattering (cf. Fig. 2). The increase in $\mathrm{Re}\Delta_N$ due to resonant depairing by Kondo impurities is thus analogous to the decrease in $\mathrm{Re}\Delta_N$ arising from resonant pairing via phonon scattering. For resonant depairing, one observes that beyond the resonant energy, $\mathrm{Re}\Delta_N$ can be enhanced to a value even *greater* than the S metal gap. This apparent "over compensation" is necessary in order to force the quasiparticle density of states (cf. Fig. 3) back to zero and reestablish the superconductivity of an ordinary N-S sandwich. The other unique feature of Kondo impurities in the N metal of a thin N-S sandwich is the fact that the resonant scattering energy, $y_0\Delta_S$, is tied to the S-metal energy gap, and is not uniquely fixed by the properties of the impurities in the N metal.

The tunneling densities of states corresponding to the pair potentials of Fig. 2 are plotted in Fig. 3. The main features of $N_T(E)$ here is the "bound state" which develops around $E=y_0\Delta_S$. This corresponds exactly to the region of negative $\mathrm{Im}\Delta_N(E)$ discussed above. As the impurity concentration increases, the bound state broadens and grows in height, taking density initially from the gap edge primarily, but also from the high-energy side of the main peak in N_T. The dip at $E=\Delta_S$ is due to the proximity effect itself, and is present even for the pure metals treated in PE I. This dip has been observed by Wolf *et al.*,[13] and was used to obtain a value for the energy gap in the S metal. This dip broadens as d_N increases, but ordinarily would be unobservable above temperatures of a few tens of millikelvins, unless a superconducting counter electrode is used (in this paper, we assume a normal-metal counter electrode). Unlike the bulk case, the bound state never actually merges with the continuum, but the gap between it and the continuum becomes quite narrow for large concentrations.

B. Variation of $N_T(E)$ with y_0 for fixed concentration

In Fig. 4 we investigate the variation of the tunneling density of states with y_0. Again, we take $R=0.0484$, $Z_N^{\mathrm{ph}}=1.2$, $\Delta_N^{\mathrm{ph}}=0.3$, and $\Delta_S=1.20$. We have adjusted d/l_2 according to Eq. (2.8) so as to keep the impurity concentration constant. The concentration was arbitrarily chosen so that $d/l_2=0.006$ at $y_0=0.7$. As a concrete example, this would give $c\cong 20$ ppm for a copper N metal. At $y_0=0.1$ we see the bound state is flattened against the line $E=0$. As y_0 increases, it moves to higher energy and takes on a parabolic shape. For y_0 close to 0.1, it becomes narrower and higher, eventually flattening itself against the main peak in the density of states. For all y_0, the area of the bound-state peak is substantially unchanged, though d/l_2 ranges from 0.570 to 0.001 as y_0 varies from 0.1 to 0.9. That is, the area of the bound state is approximately constant with y_0 for constant c.

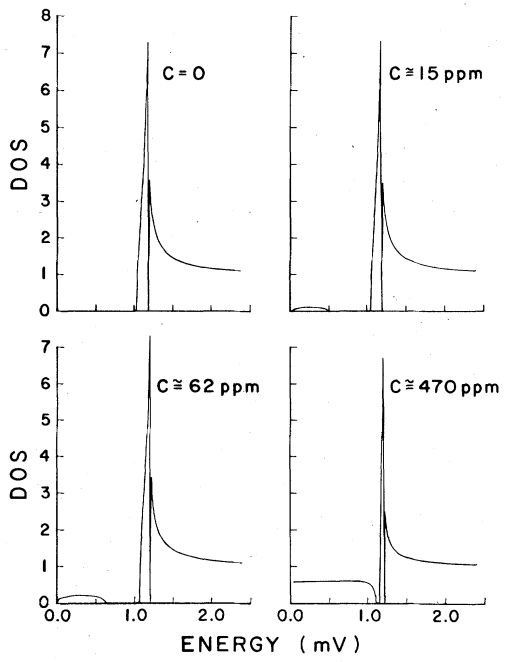

FIG. 3. Normalized tunneling densities of states obtained from the pair potentials in Fig. 2.

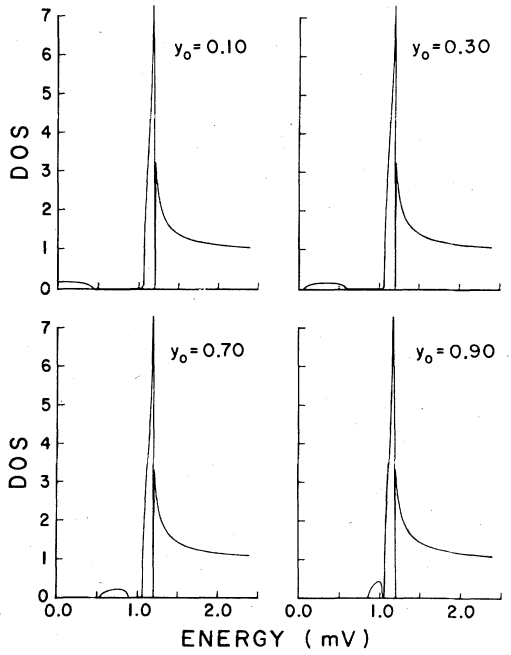

FIG. 4. Normalized density of states as a function of y_0 for fixed concentration. This corresponds to 250 Å of copper with an impurity concentration $c\sim 20$ ppm.

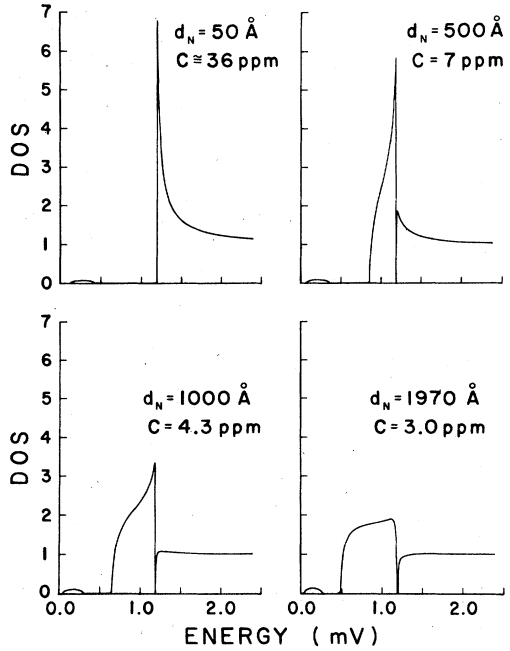

FIG. 5. Normalized density of states versus N metal thickness for constant $y_0=0.23$. (Note the three gaps in the density of states at large thicknesses.)

C. Variation of $N_T(E)$ with thickness for constant y_0

In Fig. 5, we present the variation of N_T with the N-metal R ($R=2d/\hbar v_F$). We have chosen $\Delta_S=1.2$, $y_0=0.23$, $\Delta_N^{\rm ph}=0.3$, and $Z_N^{\rm ph}=1.20$. The value of c was decreased slightly as R increased to keep the bound-state area constant. The R values shown range from 0.01 to 0.38, which for copper would correspond to thicknesses from about 50 to 1970 Å.

We see that for small R, the density of states is quite BCS-type, but with the bound state appended. As R increases, density flows from the continuum into the proximity-effect band below Δ_S, as discussed in PE II. As the proximity-effect band widens, it feeds density into the high-energy side of the bound state (which is why we had to decrease c to keep the area constant). It also takes density from the continuum, and the gap at $E=\Delta_S$ broadens. It is amusing to note that for the largest values of R illustrated there should be not two, but *three* gaps observable in the density of states. For values of R larger than those illustrated, the gap at Δ_S closes in again and the density of states becomes just that of a normal metal.

VI. COMPARISON WITH EXPERIMENT

We intend here to test our theory against experimental results, specifically those of Ref. 14, which will hereafter be called DGN. The part of DGN most relevant to our theory is the study of thin Cu-Cr films in proximity to thick (2000 Å) Pb films. We expect evaporated films, such as those of DGN, to contain many defects which should behave as nonmagnetic scattering centers so that Eqs. (4.1) and (4.2) for the pair potential and renormalization function should be applicable even for small concentrations of the magnetic impurities. Lacking a theory of the proximity effect, DGN assumes that N-S sandwiches behave as BCS superconductors. When the S metal is thick, this is true only for extremely thin N metals. As the N metal becomes thicker, the BCS approximation loses validity.

In fitting our theory to the data, we had to adjust Δ_S, y_0, and the impurity concentration c. In adjusting Δ_S, our first impulse was to use a theoretical approximation $\Delta_S=\Delta_{S_0}(1-\pi R\Delta_{S_0})$ [see Eqs. (8.4)–(8.6) of PE I]. However, we found that even for the case of a pure copper N metal, this equation overestimated the depression of Δ_S. This is easy to understand if the N metal is full of nonmagnetic scattering centers. The above equation (6.1) was derived for perfectly clean metals and assumed that $\Delta_N=0$, but impurities or defects will scatter electrons back into the S metal, so that they sample the large pair potential there more often. This will lead to an induced Δ_N and, consequently, less depression of Δ_S.

An analysis of DGN's data for a pure copper N metal at 1 K still yields a relationship similar to the above equation. We find $\Delta_S\cong\Delta_{S_0}(1-0.57\pi R\Delta_{S_0})$. Though it is gratifying to see that the relationship for $\Delta_N=0$ is close to the empirically correct one, we shall only note it and not use, it further. We shall estimate Δ_S from experiments to be that value which reproduces the position of the peak in the density of states when the N metal has *no* magnetic impurities. We shall neglect the variation of Δ_S with N-metal impurity concentration.

Having estimated Δ_S, we shall take y_0 to be that value which reproduces the position of the bound state at low concentrations. We shall also neglect all variations of y_0. Finally, our equations depend on the impurity concentration c only through d/l_2. We use Eq. (2.8) to estimate d/l_2 from the experimental c, assuming N_0 and v_F have their free-electron values for the host metal.

We plot our results in Fig. 6. This corresponds to Fig. 8 of DGN. The figures represent Eq. (4.14) with $\Delta_S=1.2$, $y_0=0.23$, $\Delta_N^{\rm ph}=0$, $R_N=0.0484$, $R_S=0.3322$,

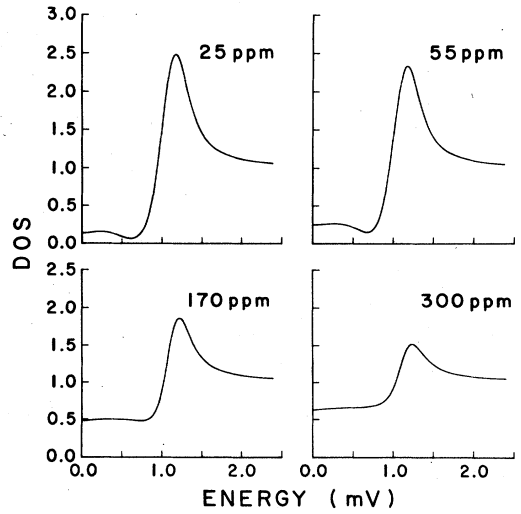

FIG. 6. Tunneling density of states versus concentration for 250 Å copper on 2000 Å Pb assuming Δ for Pb is depressed to 1.2 mV. Compare to Fig. 8 of Ref. 14.

$Z_S=1$, and as before $Z_N^{ph}=1.2$. The agreement with DGN is quite fair, much better than the BCS approximation. One quantitative deficit exists, however. Our densities of states exhibit a narrower peak near Δ_S at all impurity concentrations than do those of DGN. This may be traced to the fact that we neglected the energy dependence of $\Delta_S(E)$. The energy dependence of Δ_S would enhance that of Δ_N near $E=\Delta_S$, and so broaden the peak in question. Taking $\Delta_S(E)$ to depend on energy would require simultaneously solving Eq. (4.2) of this reference for Δ_N and (8.1) and (8.2) of PE I for Δ_S. In view of the difficulties of solving even (4.2) alone, we have not yet done this.

VII. CONCLUSION

We believe our treatment of elastic scattering in an N-S sandwich explains the experimental results obtained when the N metal contains Kondo-effect impurities. Relaxation of our assumption that much nonmagnetic scattering is occurring in evaporated films should not be necessary, as we expect energy dependence of Δ_S at the N-S interface to remedy most of the remaining deficit between experiments and theory. This energy dependence will be enhanced by the proximity effect. The complete solution for $\Delta_S(E)$ and $\Delta_N(E)$ is a subject for future study.

This paper also suggests other geometries that might possibly be studied. One might dope the S metal with Kondo impurities and leave the N metal pure. In this case, we might expect for not too thin N metals an attenuation of the bound-state amplitude in the density of states. A more interesting possibility would be to consider a case in which the N and S metals are doped with impurities having different values of y_0, y_0^N, and y_0^S, respectively. For $y_0^S > y_0^N$ and sufficiently low impurity concentrations, we might expect to see two distinct bound states due to the Kondo impurities. Thus, with the proximity effect gap near $E=\Delta_S$, there would be a total of four gaps in the tunneling density of states. For $y_0^S \leq y_0^N$ the qualitative picture is not so clear and is also a subject for future numerical study.

Thus far, we have assumed that Kondo-effect impurities behave in superconducting thin films just as they do in bulk S metals. Though this assumption seems justified by the agreement between the results of this paper and experiments, a reworking of the Green-function theory for thin films instead of bulk metals may be desirable. More desirable would be the adaptation of the exact solution of the Kondo problem[15] to the case in which the host metal is a superconductor.

ACKNOWLEDGMENTS

This research was supported by National Science Foundation Grant No. DMR-80-19739.

[1]S. Yoksan, J. Low Temp. Phys. **51**, 569 (1983).
[2]I. M. Tang and S. Roongkeadsakoon, J. Low Temp. Phys. **51**, 67 (1983).
[3]G. B. Arnold, Phys. Rev. B **18**, 1076 (1978).
[4]G. B. Arnold, Phys. Rev. B **23**, 1171 (1981).
[5]K. Maki, in *Superconductivity,* edited by R. Parks (Dekker, New York, 1969), p. 1035.
[6]J. Zittartz, A. Bringer, and E. Müller-Hartmann, Solid State Commun. **10**, 513 (1972).
[7]J. Zittartz and E. Müller-Hartmann, Z. Phys. **232**, 11 (1969).
[8]J. Zittartz and E. Müller-Hartmann, Z. Phys. **234**, 58 (1970).
[9]J. Zittartz, Z. Phys. **237**, 419 (1970).
[10]E. Müller-Hartmann, in *Magnetism V,* edited by H. Suhl (Academic, New York, 1973), p. 367.
[11]International Mathematics and Scientific Library routine ZCPOLY. Copyright by IMSL, Inc. (1978).
[12]W. J. Gallagher, Phys. Rev. B **22**, 1233 (1980).
[13]E. L. Wolf, R. J. Noer, and G. B. Arnold, J. Low Temp. Phys. **40**, 419 (1980).
[14]L. Dumoulin, E. Guyon, and P. Nedellec, Phys. Rev. B **16**, 1086 (1977).
[15]N. Andrei, K. Furuya, and J. H. Lowenstein, Rev. Mod. Phys. **55**, 2 (1983).